Numerical Analysis of Tip Clearance Effects in a Micro Radial Inflow Turbine

Naoki WATANABE, Susumu TERAMOTO, Toshio NAGASHIMA

Department of Aeronautics and Astronautics, University of Tokyo
7-3-1 Hongo, Bunkyo-ku, Tokyo 113-8656, JAPAN
E-mail: naoki@thermo.t.u-tokyo.ac.jp

Keywords: ultra-micro gas turbine, radial inflow turbine, tip clearance

Abstract

There are many difficulties in realizing Ultra-micro gas turbine system. Among them, the effects of tip clearance upon the micro turbine flowfield are discussed in this paper. The flowfield was investigated numerically with the Reynolds-averaged three-dimensional thin-layer Navier-Stokes equations. Calculations were conducted with clearance height from 0% to 10% of the passage height. Leakage mass flow and deterioration of efficiency are proportional to the clearance height for the clearance height larger than 4%. However, in the case of 2% clearance, leakage flow is significantly reduced due to relative motion of the casing and as a result deterioration of efficiency is very small. It is difficult to control tip clearance in micro turbines, but the results of this study indicate that if the clearance height is controlled within a few percent of passage height, deterioration of stage performace will be small.

Introduction

There has been many efforts to minimize gas turbine, aiming application to portable electric power source[1]. A minimized gas turbine which we call "Ultra-micro gas turbine" will be made with MEMS(Micro Electro Mechanical Systems) technology at very low cost and have higher power density than conventional batteries

However, there are still many difficulties to be overcome before realizing such gas turbines, for example, manufacturing process, material, bearing support and combustion. For the compressor and the turbine, manufacturing process based on MEMS technology confines the blade shape in two dimensional geometry. In addition, there are several aerodynamic concerns.

- Tip Clearance
  It is very difficult to control the tip clearance in minimized gas turbines and, as the scale of aerodynamic components becomes smaller, the tip clearance becomes relatively large.

- Decrease of Reynolds number
  Relatively thicker boundary layer and laminarization due to the decrease of Reynolds number may have a large impact on the flowfield inside gas turbines.

- Heat Transfer
  The temperature of each component of the gas turbine becomes almost uniform due to very small Biot number. Temperature gradient near solid wall becomes steep and the influence of heat transfer upon the flowfield is not negligible.

The authors have studied the effects of Reynolds number and heat transfer[2]. The objective of the current study is to discuss the effects of tip clearance upon the flowfield inside a micro radial inflow turbine.

There are many papers on tip clearance published before, but most of them deal with axial turbines and very little is known about tip clearance flow in radial turbines. The best-known investigation of clearance effects on a radial turbine was undertaken by Futral and Holeski[3]. They concluded that radial clearance increases at the rotor exit have about 10 times larger effect on the overall efficiency than the axial clearance increases at the rotor inlet.

Dambach et al.[4] investigated the details of tip clearance flow in a radial turbine. Tip leakage flow is opposed by flow adjacent to the casing, which is moving from the suction side to the pressure side due to a no-slip condition at the casing. It is called "scraping flow". They revealed that due to scraping flow, radial clearance at the rotor exit is more important than axial clearance at the rotor inlet.

All the researches focused on turbines that have three dimensional blades with conventional sizes, typically centimeters or meters. In this report, the effects of tip clearance height in a micro two dimensional radial turbine are discussed based on the above results.

Target and Approach

The turbine studied in this report is a one-tenth scale model of the radial inflow turbine designed and tested by Kato et al.[5]. Table 1 shows the design characteristics. In the numerical analysis, the stage performance and the flowfield are compared for several clearance heights. Table 2 shows the calculation cases. They are referred to 0%cl, 2%cl, 4%cl, 6%cl and 10%cl respectively.

Table 1 Design characteristics

rotational speed	2,400,000 rpm
pressure ratio	2.5
mass-flow rate	0.30 g/sec
speed ratio	$U/C_0 \simeq 0.63$
inlet total temperature	1223K
specific heat ratio	1.35
gas constant	287.4 J/kg/K
Nozzle	
outer diameter	5.2 mm
inner diameter	4.2 mm
number of blades	17
blade height	0.48 mm
Rotor	
outer diameter	4.0 mm
inner diameter	2.6 mm
number of blades	15
blade height	0.48 mm

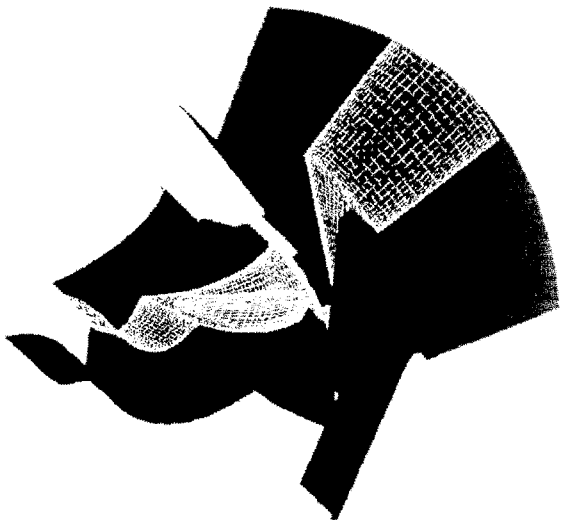

Fig. 1 Grid outline

Table 2 Calculation cases

case	clearance height	% passage height
0%cl	0 mm	0 %
2%cl	0.01 mm	2.1 %
4%cl	0.02 mm	4.2 %
6%cl	0.03 mm	6.3 %
10%cl	0.05 mm	10.4 %

U/C_0(the ratio of peripheral velocity U to theoretical isentropic expansion velocity C_0) is used as a parameter of operation condition, which is varied within the range from 0.4 to 0.8.

The stage performance will be discussed with adiabatic efficiency η_{ad} defined as follows,

$$\eta_{ad} = \frac{W}{\dot{m}C_p T_{01}\{1 - (\frac{p_3}{p_{01}})^{\frac{\gamma-1}{\gamma}}\}} \quad (1)$$

where suffix 0, 1, and 3 represent stagnation condition, nozzle inlet, and rotor outlet respectively. W represents the turbine work output, which is evaluated by integrating pressure and shear stress over the rotor blade.

Numerical Method

The governing equations employed here are the Reynolds-averaged three-dimensional thin-layer Navier-Stokes equations. Numerical fluxes for the convective terms are evaluated by the simple high-resolution upwind scheme (SHUS)[6], which is extended to higher order by the MUSCL interpolation based on the primitive variables. The lower-upper alternating directional implicit (LU-ADI) factorized implicit algorithm[7] is employed for time integration.

Reynolds number is 10^3 to 10^4. The flowfield is thus considered to be laminar and no turbulence model is applied.

Outline of the computational grid used in the simulation is illustrated in Fig.1. Though the figure illustrates three pitches, the simulation area is one pitch of blade to blade passage. The grid is $88 \times 35 \times 35$ for the nozzle and $83 \times 35 \times 35$ for the rotor with H-H topology. The minimum grid spacing near the wall is $1.0 \times 10^{-7} m$, so that y^+ is less than unity. Grid for the tip clearance region between the rotor and the casing is $51 \times 34 \times 19$: 2%cl, $51 \times 34 \times 21$: 4%cl, $51 \times 34 \times 23$: 6%cl and $51 \times 34 \times 25$: 10%cl respectively, and the clearance grid is embedded into the rotor grid. The dimension of the grid is decided so that the minimum grid spacing coincides with that of the rotor grid.

At the nozzle inlet boundary, total pressure and total temperature are fixed and flow angle is given as radial inflow. At the exducer outlet boundary, static pressure distribution is given by assuming simple radial equilibrium. The blade surface and hub surface of the rotor are rotating around the axis and no-slip adiabatic wall condition is applied over all solid walls. Periodic condition is applied for the pitchwise boundaries other than the blade surfaces.

At the zonal interface between the nozzle and the rotor, grid lines are overlapped by three points and the mixing plane method is applied, in which physical quantities are averaged in the pitchwise direction and exchanged between two zones. Steady analysis is carried out with this method. At the interface between the main passage and the tip clearance, several grid points are overlapped around the gap region (Fig.2). At the boundary of the tip clearance zone physical quantities are interpolated from the main passage and at the grid points of the main passage which is contained inside

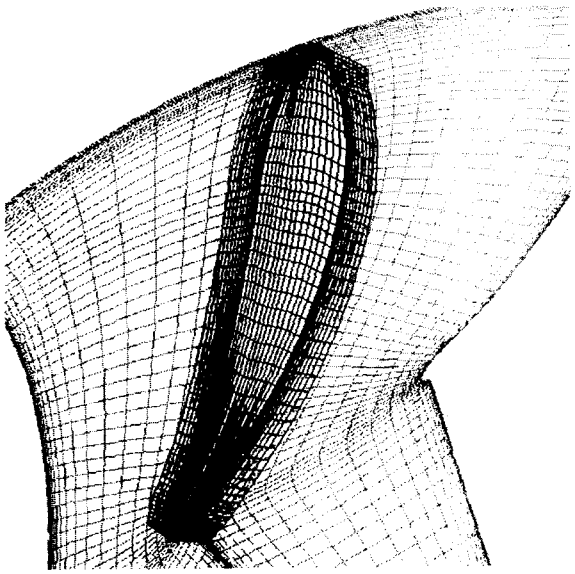

Fig. 2 Zonal interface between the main passage and the tip clearance

the tip clearance zone physical quantities are interpolated from the tip clearance zone.

Results and Discussion

Overview of Leakage Flow

First, overview of leakage flow is presented. $U/C_0 = 0.6$ of 6%cl is taken as a representative case. Figure 3, 4 and 5 show relative velocity vectors and vorticity contours at 13%, 32% and 57% chord respectively. Velocity vectors at left top and right top of Fig.3 indicate that leakage flow already exists at 13% chord. The leakage flow is also observed from the vorticity contour.

At 32% chord, the velocity vectors induced by the leakage flow reach the pressure side of the adjacent blade. As a result, the area of high vorticity is formed at the inlet and the outlet of the tip clearance, and near the casing.

At 57% chord, the leakage flow begins to form leakage vortex and area of high vorticity spreads out to the center of the passage. The stream in the upper region of the passage grows larger.

Effect of tip clearance height

In this section, effect of tip clearance height is discussed. Figure 6 shows adiabatic efficiency plotted against U/C_0 for each case. Deterioration of efficiency caused by the tip clearance height is observed from the figure. Larger tip clearance produces larger loss, but the deterioration of 2%cl is much less than those of other cases.

Flowfields at $U/C_0 = 0.6$ (near the design point) for each clearance height is discussed in detail hereafter. Figure 7 shows leakage mass flow rate for each case,

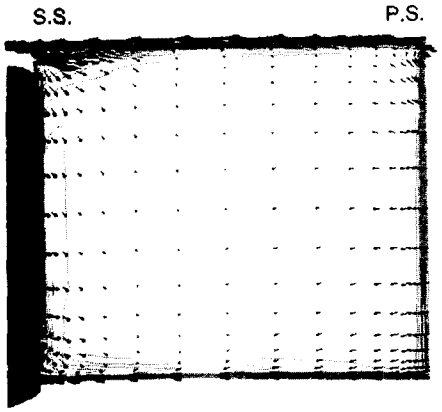

Fig. 3 secondary flow at 13% chord (6%cl, $U/C_0 = 0.6$)

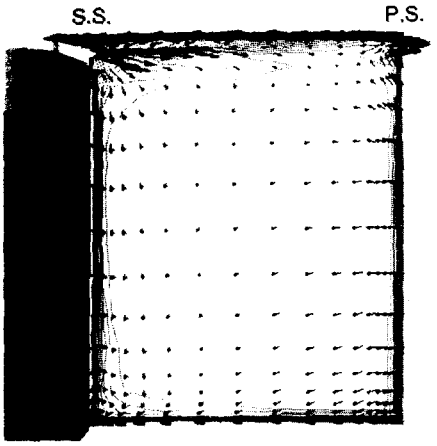

Fig. 4 secondary flow at 32% chord (6%cl, $U/C_0 = 0.6$)

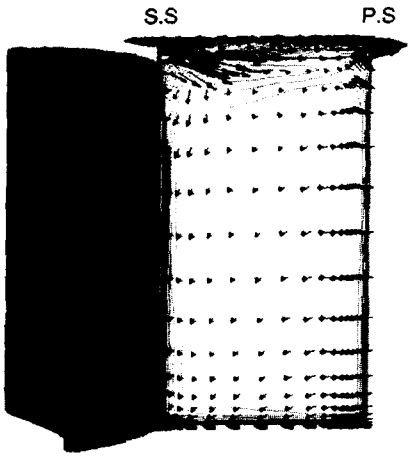

Fig. 5 secondary flow at 57% chord (6%cl, $U/C_0 = 0.6$)

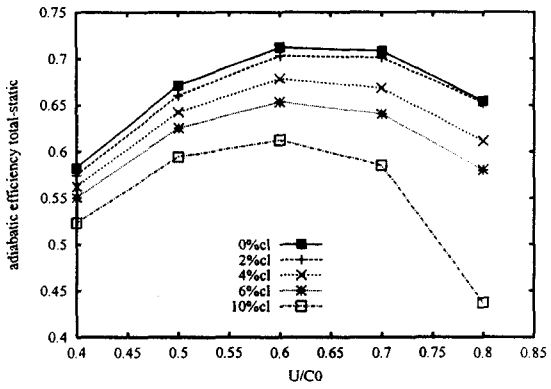

Fig. 6 Adiabatic efficiency

which is calculated by integrating mass flow entering into the main stream through the suction surface from the leading edge to each position as the upper figure shows.

$$Q_L(x) = \int_{L.E.}^{x} \int_{tip}^{casing} \rho \vec{u} \cdot d\vec{S} \qquad (2)$$

where ρ, $\vec{u}$ and $d\vec{S}$ are density, velocity vector and area vector of local cell respectively. Positive Q_L means the fluid inside the clearance flows from the pressure side to the suction side. This figure indicates that leakage mass flow rate also correlates with tip clearance height, but that at 2%cl is almost zero. These results reveal that the deterioration of efficiency correspond to the leakage mass flow rate.

Flowfield in the tip clearance region is discussed in the following. Figure 8 shows velocity vectors at the mid-gap section (94% span) for 10%cl. Figure 9 shows surface pressure distribution of the blade at 94% span for 0%cl. These figures show that leakage flow from the pressure side to the suction side is induced by the pressure differences at the whole chord position.

Figure 10 and 11 also show velocity vectors at the mid-gap section (99% span) for 2%cl and surface pressure distribution at 99% span for 0%cl. It is worth while to notice that the velocity vector directs from the suction side toward the pressure side near the leading edge. The pressure at the suction surface is higher than that at the pressure surface and the flow is driven by this pressure difference. As pressure of the suction surface drops, the flow is turned to the opposite direction. This flowfield results in small leakage mass flow rate for 2%cl.

Scraping flow

The pressure rise of the suction surface for 2%cl is explained by scraping flow which is induced by relative motion of the casing.

Two characteristic features of the turbine studied in this article should be emphasized.

- Very low Reynolds number

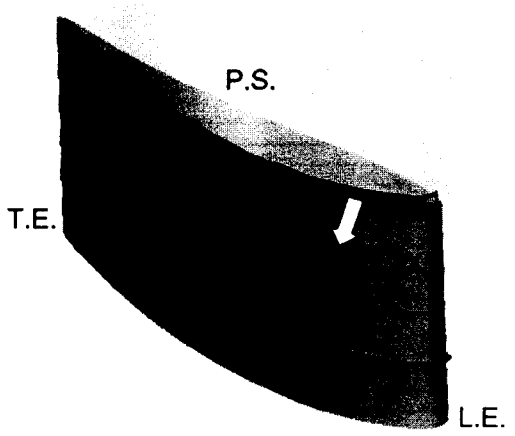

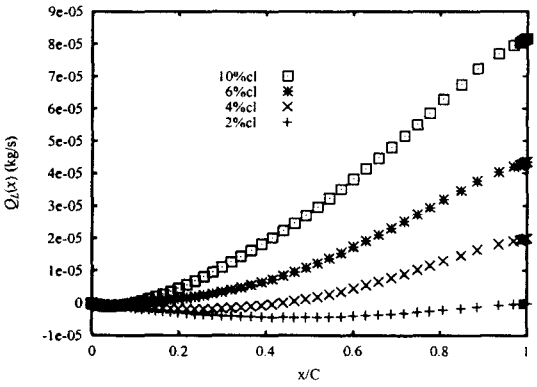

Fig. 7 Leakage mass flow

- Radial turbine

First, very low Reynolds number enhances viscosity effect. It means that the casing drags fluid at the tip region and it induces strong scraping flow. Second, the circumferential velocity of a radial turbine varies with the radius. Relative motion of the casing and strength of the scraping flow also varies with the radius.

Dambach et al.[4] explained tip gap flow of a radial turbine with "scraping ratio" defined by the following equation.

$$R = \frac{\Delta p}{\frac{1}{2}\rho U^2 \cos^2 \gamma} \qquad (3)$$

In this equation, Δp is the pressure difference between both sides of the blade, ρ is the density near the casing and $U \cos\gamma$ is the casing relative velocity perpendicular to the blade surface. They concluded that clearance jet induced by the effect of pressure difference is dominant at the tip region when the scraping ratio is large, while scraping flow is dominant when the scraping ratio is small.

Scraping ratio for $U/C_0 = 0.6$ of 2%cl is shown in Fig.12, where pressure difference at the midspan is taken as Δp. The flowfield shown in Fig.10 is explained with this plot. Scraping flow near the leading edge is strong since the casing moves faster at the region and thus the fluid inside the clearance flows from

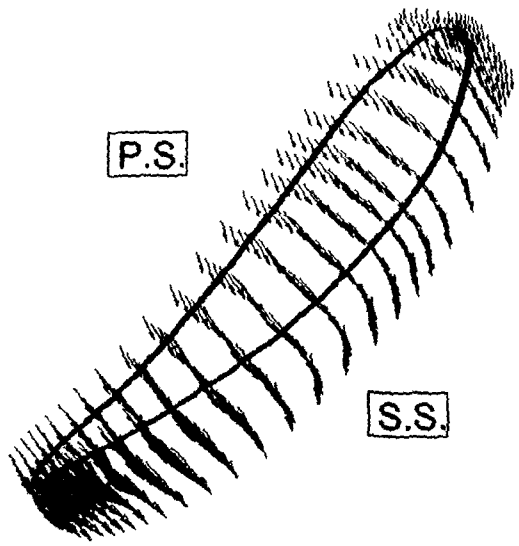

Fig. 8 Velocity distribution at 94% span (10%cl, $U/C_0 = 0.6$)

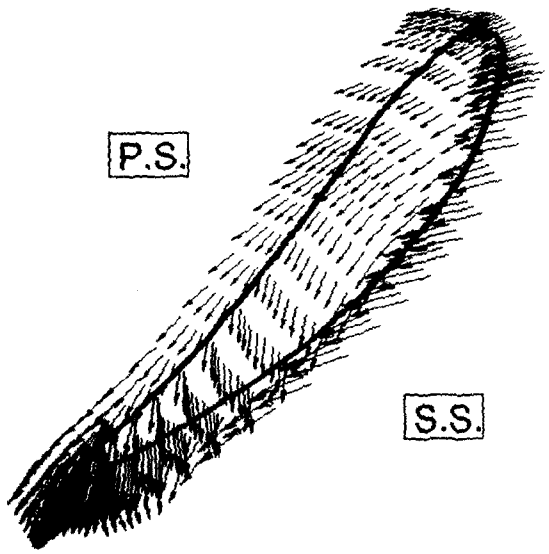

Fig. 10 Velocity distribution at 99% span (2%cl, $U/C_0 = 0.6$)

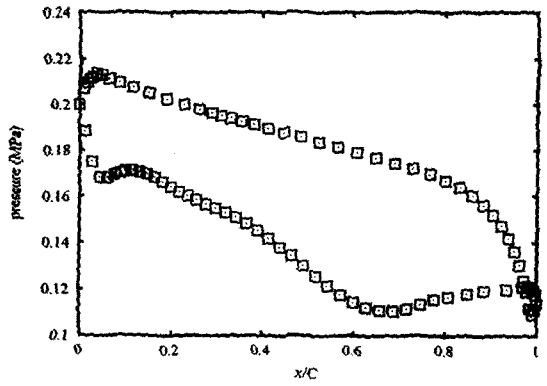

Fig. 9 Pressure distribution at 94% span (0%cl, $U/C_0 = 0.6$)

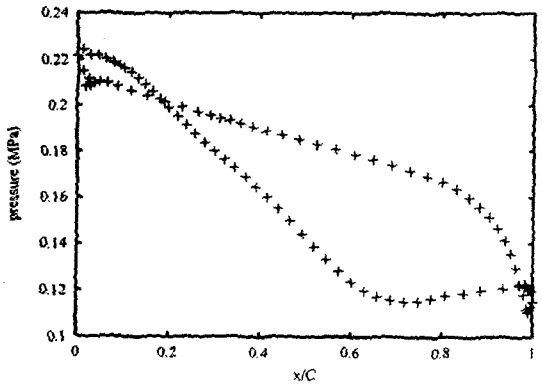

Fig. 11 Pressure distribution at 99% span (0%cl, $U/C_0 = 0.6$)

the pressure side to the suction side. Meanwhile, the scraping ratio becomes much larger with the decrease of the radius and the pressure difference becomes dominant at the rear half of the blade. Flow is turned to the opposite direction.

In 2%cl, great portion of the tip gap is contained within the area affected by the scraping flow. Therefore, pressure difference and scraping flow determine the flowfield of the tip clearance region. In the other cases, great portion of the tip gap is out of the area affected by the scraping flow and the flowfield of the tip clearance region is dominated by pressure difference only. This is the reason why 2%cl has a specific feature on efficiency and leakage mass flow rate.

These results indicate that small tip clearance comparable to 2% passage height hardly deteriorate the stage performace because leakage flow is significantly reduced by scraping flow.

Conclusions

Effects of tip clearance on the flowfield inside a micro radial inflow turbine were numerically investigated. Calculations were conducted with clearance height from 0% to 10% of the passage height. Leakage mass flow and deterioration of efficiency are proportional to the clearance height for the clearance height larger than 4%. However, in the case of 2% clearance, leakage flow is significantly reduced due to relative motion of the casing and as a result deterioration of efficiency is very small.

Scraping flow induced by the relative motion of the casing acts as a blockage to the leakage flow. In micro scale turbines, viscosity effect is strong due to very low Reynolds number. Therefore scraping flow becomes stronger than in conventional scale turbines. In addition, the circumferential velocity of a radial turbine varies with the radius. Relative motion of the casing

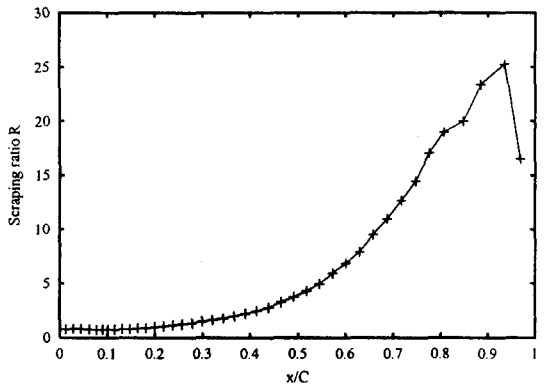

Fig. 12 Scraping ratio (2%cl, $U/C_0 = 0.6$)

and strength of scraping flow also varies with the radius. It means scraping flow is strong near the leading edge. In the case of 2% clearance, great portion of the tip gap is contained within the area affected by the scraping flow and for this reason, leakage flow is significantly reduced.

It is difficult to control tip clearance in micro turbines, but these results indicate that if the clearance height is controlled within a few percent of passage height, deterioration of stage performace will be small.

Acknowledgments

The present work was financially supported by NEDO International Joint Research Project (FY2001 No.5110159-0 and FY2002 No.0106013). The investigation is cooperated under a provisional committee of GTSJ for studying the minimization of gas turbine system.

References

1) Epstein, A. H., et al., "Micro-Heat Engines, Gas Turbines, and Rocket Engines", AIAA 97-1773

2) Watanabe, N., Teramoto, S., and Nagashima, T., "Numerical Analysis of 2.5 Dimensional Geometry Turbine Performance", Proceedings of International Gas Turbine Congress 2003 Tokyo

3) Futral, S. M., and Holeski, D. E, 1970, "Experimental Results of Varying the Blade-Shroud Clearance in a 6.02-inch Radial Inflow Turbine," NASA Technical Note D-5513.

4) Dambach, R., Hodson, H. P., and Huntsman, I., 1999, "An Experimental Study of Tip Clearance Flow in a Radial Inflow Turbine," ASME J. Turbomach., 121, pp. 644-650.

5) Matsuura, K., Kato, C., Yoshiki, H., Matsuo, E., Ikeda, H., Nishimura, K., and Sapkota, R., "Prototyping of Small-sized Two-dimensional Radial Turbines", Proceedings of International Gas Turbine Congress 2003 Tokyo

6) Shima, E., and Jounouchi, T., "Role of CFD in Aeronautical Engineering (No.14)-AUSM Type Upwind Schemes", Proceedings of the 14th NAL Symposium on Aircraft Computational Aerodynamics, National Aerospace Lab., NAL SP-34, Tokyo, 1997, pp.7-12.

7) Obayashi, S., Matsushima, K., Fujii, K., and Kuwahara, K., "Improvements in Efficiency and Reliability for Navier-Stokes Computations Using the LU-ADI Factorization Algorithm", AIAA Paper 86-0338, Jan. 1986.